

Optimal Adaptive Fuzzy Integral Sliding Model Control for Electrically Driven SCARA Robot Manipulator

Mohammad Reza Soltanpour^{1*}, Pooria Otadolajam², Mahmoodreza Soltani³

Received:2015/6/25

Accepted:2015/9/1

Abstract

In this paper, an optimal adaptive fuzzy integral sliding mode control is presented to control the robot manipulator position tracking in the presence of uncertainties and permanent magnet DC motor. In the proposed control, sliding surface of the sliding mode control is defined according to the information of position tracking error, derivatives, and error integral. In order to estimate bounds of the existing structured and unstructured uncertainties in the dynamics of the robot manipulator and the permanent magnet DC motor, a MIMO fuzzy adaptive approximator is designed. This helps to overcome the undesired chattering phenomenon in the control input by using fuzzy logic. Mathematical proof shows that the closed-loop system with the adaptive fuzzy integral sliding mode control in the presence of all the uncertainties has the global asymptotic stability. Furthermore, modified harmony search optimization algorithm is used to define the input coefficients of the proposed control and also to reduce the control input amplitude. In order to validate performance of the proposed controller, a case study on the SCARA robot manipulator is conducted in the presence of permanent magnet DC motor. Results of the Simulation show desired performance of the proposed controller.

Keywords: Robot Manipulator, Structured and Unstructured Uncertainties, Integral Sliding Mode Control, Optimal Adaptive Fuzzy Integral Sliding Mode Control, Electrically Driven.

1. Introduction

Robot manipulator is a nonlinear system

Thus, dynamic control of the robot manipulator is very important. Large numbers of couplings are used between the joints in structure of the robot

manipulator. Respectively in coupling of the actuators to the joints, coupling of the joints to the interfaces, dynamic and static frictions in each joint requires accurate and complex modeling to control of robot manipulator with high precision. However, there are many problems in the practical implementation of the controllers, based on the actual model of the system. Moreover, even if this ability exists in the model, actual model of the system is too complicated that makes it difficult to design the controller. These problems cause imprecision in the model. Such imprecision in the model also causes structured and unstructured uncertainties. Thus, to overcome the structured and unstructured uncertainties, robot manipulator control requires a robust controller [1]. In recent years, different controllers have been presented to deal with these uncertainties. Sliding mode control is a robust controller that has been used to control the systems which consists of uncertainties. However, there is a damaging factor in sliding mode controller, which is called chattering. This phenomenon appears due to nature of the sliding mode controller which is a switching controller [2]. Although, this factor endangers performance of the robot manipulator control, it has been applied widely [3-6]. To reduce damaging effects of the chattering in the sliding mode control some methods have been presented. Among these methods, there have been some applications of saturation function, low-pass filter [3-6] and fuzzy systems [7-8], that each one has some problems. Saturation function and low-pass filter cause the reduction of chattering in control input. To some extent, steady-state error is increased in the position of the robot manipulator joints and it is not easy to prove the asymptotical stability of the sliding mode controller. This phenomenon is reduced through the use of fuzzy systems. However, researchers have used too many rules in fuzzy system rule base for further reduction of chattering and steady-state error in the robot manipulator position tracking control in the presence of structured and

1.*Department of Electrical Engineering ShahidSattari Aeronautical University of Science and Technology, Tehran, Iran, m_r_soltanpour@yahoo.com.

2. Department of Electrical and Control Engineering, Faculty of Engineering, Garmsar Branch, Islamic Azad University, Garmsar, Iran, pooria.otad@gmail.com

3 . Glenn Department of Civil Engineering Clemson University, Clemson, SC, USA, msoltan@clemson.edu

unstructured uncertainties. This leads to a massive computational load. Consequently, for practical implementation of these controllers, applications of high-speed processors are inevitable and in many cases, application of these fuzzy systems is impractical. To overcome the mentioned problems, the researchers have presented the adaptive fuzzy sliding mode controllers. However, all the adaptive fuzzy sliding mode controllers have different behaviors due to the design type of sliding mode algorithm, the type of fuzzy system, the approximation of fuzzy system factor, and the adaptive law. In general, the adaptive fuzzy sliding mode controllers are divided in two categories, direct adaptive fuzzy sliding mode control and indirect adaptive fuzzy sliding mode control. In the direct adaptive fuzzy sliding mode control, control input coefficients are tuned by using online adaptive law to reduce the tracking error [9-10]. In the indirect adaptive fuzzy sliding mode control, the system parameters could be tuned according to approximation of the system dynamics and by adaptive law to reduce the tracking error [11-16]. In adaptive fuzzy sliding mode controller [12], the MIMO fuzzy system is used to approximate the uncertainties existing in the dynamical equations of the robot manipulator by using position, velocity, and acceleration information of the robot manipulator joints. This controller has high computational load and due to nonlinear switching function in control input, has difficulties to encounter with chattering phenomenon. Thus, practical implementation of the proposed control is impossible. Using the MIMO fuzzy system in adaptive fuzzy sliding mode controller [16], existing uncertainties in the robot manipulator dynamic equations is approximated. Additionally, according to sliding surface information, dynamic of inertial matrix is presented and at the same time approximates the switching function with SISO fuzzy system. This controller due to the use of several adaptive laws in its control input has high computational load and by occurrence of delay in calculation of the control input, it is impossible to guarantee the closed-loop system stability.

In adaptive fuzzy sliding mode controller [14], an approximate of the switching function by using SISO fuzzy system based on sliding surface information has been presented. The presented control has a low computational load. This factor has a suitable influence on the operation processing pace of robot manipulator. However in the design of SISO fuzzy system, interaction influence of robot manipulator joints in the robot manipulator position tracking control has not been considered. For this reason, robot manipulator control in high-speed operations is difficult.

Adaptive law has been obtained based on Lyapunov stability proof for all the presented adaptive fuzzy sliding mode controllers for tracking the position of the robot manipulator. For practical implementation of these controllers, sliding surface information must be available. To determine the sliding surface of these controllers only information of error and its derivatives have been used, tracking error converges toward zero slowly. Hence, the tracking accuracy in robot manipulators that have high speed is reduced. On the other hand, in all adaptive fuzzy sliding mode controllers of robot manipulator, the control input has been designed in torque space. Additionally, the control of robot manipulator joints is performed through the drivers, especially electrical drivers. However, to design such controllers, the dynamic effects of these drivers are not considered. Thus the stability of the closed-loop system using the proposed controller cannot be easily guaranteed. In this paper, to overcome the problems in the adaptive fuzzy sliding mode position tracking control for a robot manipulator, the following solutions are available:

- Increase accuracy of the robot manipulator position tracking by increasing the speed of tracking error toward zero.
- Prevent occurrence of chattering phenomenon in the control input.
- Remove influence of the robot manipulator joint interactions in adaptive fuzzy sliding mode position tracking control.
- Overcome the existing uncertainties of the robot manipulator driving dynamics.
- Prevent saturation of the driving robot manipulator.
- Choose optimized coefficients for input control.

Sliding surface, which is a function of the tracking error, derivative, and error integral, is used to achieve the mentioned aims. In this case, there is an extended control for the robot manipulator position tracking error. Furthermore, to remove the robot manipulator joints interaction in the position tracking control and to prevent the occurrence of chattering in the control input, a MIMO fuzzy system is used. Finally, to overcome the existing uncertainties in the robot manipulator and the permanent magnet DC motor dynamic, using Lyapunov stability theory, the adaptive fuzzy sliding mode control is presented. This control makes the closed-loop system in the presence of all the uncertainties to have global asymptotic stability. In the proposed control, there is a coefficient that prevents increment of the control input amplitude. This causes elimination of saturation of the robot manipulator drivers. Furthermore, to achieve an optimized control input, all the control input coefficients are defined through the modified harmony search optimization algorithm. In the

proposed control design strategy, some solutions are presented that makes the proposed control more robust against the existing uncertainties.

2. The Dynamic Equations of The Robot Manipulator in The Presence of a Permanent Magnet DC Motor

The dynamic equation of the robot manipulator in the presence of Permanent Magnet DC Motor (PMDC) is as follows [17]:

$$M(q)\ddot{q} + C(q, \dot{q})\dot{q} + G(q) + F_d\dot{q} + B\dot{q} + F_s + \tau_{dl} = KV(t) \quad (1)$$

where $q \in R^n$ is vector of the robot manipulator joint position; $\dot{q} \in R^n$ is vector of the robot manipulator joint velocity and $\ddot{q} \in R^n$ is the robot manipulator joint acceleration. $M(q) \in R^{n \times n}$ is the positive definite inertia matrix, $C(q, \dot{q}) \in R^{n \times n}$ is the coriolis matrix and centrifugal forces, $G(q) \in R^n$ is the gravity vector, $F_d \in R^{n \times n}$ is the diagonal matrix of dynamic friction, $B \in R^{n \times n}$ is the diagonal matrix of effective damping PMDC motor, $F_s \in R^n$ is the vector of static friction, $\tau_{dl} \in R^n$ is the vector of disturbance and un-modeled dynamics, $V(t) \in R^n$ is the vector of amplifiers input voltage and $K \in R^{n \times n}$ is the matrix of diagonal transfer that transfers the actuators input to torque space of the robot manipulator.

Remark 1: In Eq. (1), τ_{dl} is the total existing disturbance in the robot manipulator dynamic and existing disturbance in the robot manipulator driving motor dynamic. In other words, we have:

$$\tau_{dl} = \tau_d + d_m \quad (2)$$

where $\tau_d \in R^n$ is the vector of existing disturbance and un-modeled dynamics in robot manipulator and $d_m \in R^n$ is the vector of existing disturbance and un-modeled dynamic in PMDC motors.

3. Integral Sliding Mode Control

Initially, Eq. (1) based on the acceleration vector \ddot{q} is arranged as follows:

$$\ddot{q} = M(q)^{-1}[C(q, \dot{q})\dot{q} + G(q) + F_d\dot{q} + B\dot{q} + F_s + \tau_{dl}] + M(q)^{-1}KV(t) \quad (3)$$

To simplify, Eq. (3) is shown as follows:

$$\ddot{q} = F(q, \dot{q}) + D(q)u(t) \quad (4)$$

The parameter of $u(t)$, $D(q, \dot{q})$ and $F(q, \dot{q})$ are defined as follows:

$$u(t) = KV(t) \quad (5)$$

$$D(q) = M(q)^{-1} \quad (6)$$

$$F(q, \dot{q}) = -M(q)^{-1}[C(q, \dot{q})\dot{q} + G(q) + F_d\dot{q} + B\dot{q} + F_s + \tau_{dl}] \quad (7)$$

In fact by Eq. (4), inverse dynamic of robot manipulator is described in the presence of dynamic motor. For designing the controller, tracking error vector as $e = q - q_d$ is defined, which $q \in R^n$ is the

actual joints position vector and $q_d \in R^n$ is the desired joints position vector. Additionally, sliding surface vector is defined based on the tracking error, the derivative and the integral tracking error as follows [2]:

$$s(t) = \left(\frac{d}{dt} + \lambda\right)^n \int_0^t e dt \quad (8)$$

where λ is the diagonal matrix with constant and positive entries. Considering Eq. (4) is a second order equation, so in Eq. (8), n is selected equal to 2 resulted the sliding surface vector to become as follows:

$$s(t) = \dot{e} + 2\lambda e + \lambda^2 \int_0^t e dt \quad (9)$$

Remark 2: In design of sliding mode control, the purpose is to design the control input in such way that the sliding surface $s(t)$ converges toward zero. In this case, according to Eq. (9), there is a homogenous second order differential equation with constant coefficients due to error. Thus, transient robot manipulator position tracking error converges toward zero in a short time by selecting a suitable λ .

Remark 3: Since robot manipulators are engaged in doing their assignments involving with the workspace, there will be no available exact information about parameters and dynamics. Thus, in controller design for robot manipulators, overcoming against existing structured and unstructured uncertainties have a very important role. Therefore, in controller design for robot manipulators, approximated values of parameters and their dynamics are used. Then, for controller design, known or approximated values from Equation (4) can be defined as follows:

$$\ddot{q} = \hat{F}(q, \dot{q}) + \hat{D}(q)u_{sq} \quad (10)$$

where u_{sq} is the equivalent control; $\hat{F}(q, \dot{q}) \in R^n$ and $\hat{D}(q) \in R^{n \times n}$ are the estimates of $F(q, \dot{q})$ and $D(q)$, respectively. To design the sliding mode control for tracking the position of the robot manipulator, control input is chosen as follows:

$$\begin{cases} u(t) = u_{sq}(t) - u_{ps}(t) - u_s(t) \\ u(t)^T = [u(t)_1 \quad u(t)_1 \quad \dots \quad u(t)_n] \end{cases} \quad (11)$$

Remark 4: In Eq. (11), $u_s(t)$ and $u_{ps}(t)$ are chosen in a way to converge sliding surface $s(t)$ toward zero. However, $u_{sq}(t)$ is designed to keep the sliding surface $s(t)$ unchanged at the zero value. Thus, the task of the control inputs $u_s(t)$ and $u_{ps}(t)$ are different from control input $u_{sq}(t)$.

According to the mentioned points for designing $u_{sq}(t)$, derivative of Eq. (9) in respect to time is as follows:

$$\dot{s}(t) = \ddot{e} + 2\lambda\dot{e} + \lambda^2 e \quad (12)$$

Equation (12) can be rewritten as follows:

$$\dot{s}(t) = \ddot{q} - \ddot{q}_d + 2\lambda\dot{e} + \lambda^2 e \quad (13)$$

By substitution of the Equation (4) into Equation (13):

$$\dot{s}(t) = F(q, \dot{q}) + D(q)u(t) - \ddot{q}_d + 2\lambda\dot{e} + \lambda^2 e \quad (14)$$

To design $u_{sq}(t)$, sliding surface is assumed to be equal to zero, so $u_{ps}(t) = u_s(t) = 0$. To make the control input $u_{sq}(t)$ maintains the sliding surface $s(t)$ at zero value, $\dot{s}(t) = 0$ must be considered in the Eq. (14):

$$0 = F(q, \dot{q}) + D(q)u_{sq}(t) - \ddot{q}_d + 2\lambda\dot{e} + \lambda^2 e \quad (15)$$

From Eq. (15), $u_{sq}(t)$ becomes as follows:

$$u_{sq}(t) = D(q)^{-1}(\ddot{q}_d - F(q, \dot{q}) - 2\lambda\dot{e} - \lambda^2 e) \quad (16)$$

Since all the dynamics $F(q, \dot{q})$ and $D(q)$ are not completely known, the Eq. (16) is modified as follows:

$$u_{sq}(t) = \tilde{D}(q)^{-1}(\ddot{q}_d - \tilde{F}(q, \dot{q}) - 2\lambda\dot{e} - \lambda^2 e) \quad (17)$$

where $\tilde{F}(q, \dot{q})$ and $\tilde{D}(q)$ are known dynamics of $F(q, \dot{q})$ and $D(q)$, respectively.

Furthermore, for designing control input $u(t)$, inputs $u_s(t)$ and $u_{ps}(t)$ are chosen as follows:

$$\begin{cases} u_s(t) = \eta \text{sign}(s) \\ \eta = \begin{bmatrix} \eta_{11} & \dots & 0 \\ \vdots & \ddots & \vdots \\ 0 & \dots & \eta_{nn} \end{bmatrix} \\ \text{sign}(s)^T = [\text{sign}(s_1) \quad \text{sign}(s_2) \quad \dots \quad \text{sign}(s_n)] \end{cases} \quad (18)$$

$$\begin{cases} u_{ps}(t) = Ps \\ P = \begin{bmatrix} P_{11} & \dots & 0 \\ \vdots & \ddots & \vdots \\ 0 & \dots & P_{nn} \end{bmatrix} \\ s^T = [s_1 \quad s_2 \quad \dots \quad s_n] \end{cases} \quad (19)$$

where $\text{sign}(\cdot)$ is the sign function and $\eta \in R^{n \times n}$ and $P \in R^{n \times n}$ are diagonal matrices. Thus, according to Equations (11), (17), (18), and (19), the control input $u(t)$ is as follows:

$$u(t) = \tilde{D}(q)^{-1}[\ddot{q}_d - \tilde{F}(q, \dot{q}) - 2\lambda\dot{e} - \lambda^2 e] - Ps - \eta \text{sign}(s) \quad (20)$$

For designing diagonal matrices η and P and also proving the stability of the closed-loop system, Equation (20) is arranged as follows:

$$\ddot{q}_d = \tilde{F}(q, \dot{q}) + 2\lambda\dot{e} + \lambda^2 e + \tilde{D}(q)[Ps + \eta \text{sign}(s) + u(t)] \quad (21)$$

From Equations (4), (13), and (21):

$$\dot{s} = \rho_F + \rho_D u(t) - \tilde{D}(q)Ps - \tilde{D}(q)\eta \text{sign}(s) \quad (22)$$

In Eq. (22), ρ_F and ρ_D values are defined as follows:

$$\rho_F = F(q, \dot{q}) - \tilde{F}(q, \dot{q}) \quad (23)$$

$$\rho_D = D(q) - \tilde{D}(q) \quad (24)$$

Remark 5: According to Equations (23) and (24), ρ_F and ρ_D are estimation error of $F(q, \dot{q})$ and $D(q)$, respectively.

Simplifying Eq. (22):

$$\dot{s} = \rho + \rho_D u(t) \quad (25)$$

$$\dot{s} = \rho - \tilde{D}(q)Ps - \tilde{D}(q)\eta \text{sign}(s) \quad (26)$$

Remark 6: Equation (25) shows that ρ contains all the existing structured and unstructured uncertainties in robot manipulator dynamics. In other words, if all the dynamics of the robot manipulator are completely known, thus $\rho = 0$.

Additionally, for proving stability of the closed-loop system, Lyapunov function candidate is presented as follows:

$$\begin{cases} V = \frac{1}{2} s^T s \\ s^T = [s_1 \quad s_2 \quad \dots \quad s_n] \end{cases} \quad (27)$$

Take the derivative of the Lyapunov function in respect to time:

$$\dot{V} = \frac{1}{2} \dot{s}^T s + \frac{1}{2} s^T \dot{s} = s^T \dot{s} \quad (28)$$

Then Eq. (26) is inserted in Eq. (28):

$$\dot{V} = s^T [\rho - \tilde{D}(q)Ps - \tilde{D}(q)\eta \text{sign}(s)] \quad (29)$$

In this section, the inverse inertial matrix of the robot manipulator, matrix $\tilde{D}(q)$, is expressed as follows:

$$\begin{cases} \tilde{D}(q) = \begin{bmatrix} \tilde{D}(q)_{11} & \dots & \tilde{D}(q)_{1n} \\ \vdots & \ddots & \vdots \\ \tilde{D}(q)_{n1} & \dots & \tilde{D}(q)_{nn} \end{bmatrix} \\ H(q)_j = \sum_{i=1}^n s_j \tilde{D}(q)_{ji} \\ j = 1, \dots, n \\ H(q) = [\sum_{i=1}^n s_1 \tilde{D}(q)_{1i} \quad \sum_{i=1}^n s_2 \tilde{D}(q)_{2i} \quad \dots \quad \sum_{i=1}^n s_n \tilde{D}(q)_{ni}] \\ H(q) = [H(q)_1 \quad H(q)_2 \quad \dots \quad H(q)_n] \end{cases} \quad (30)$$

And consider that, $H(q) \in R^{1 \times n}$.

From Equations (29) and (30):

$$\begin{aligned} \dot{V} &= s^T \rho - s^T \tilde{D}(q)Ps - H(q)\eta \text{sign}(s) \\ &= \sum_{j=1}^n (s_j \rho_j - H(q)_j \eta_{jj} \text{sign}(s_j)) - s^T \tilde{D}(q)Ps \end{aligned} \quad (31)$$

Equation (31) shows if $s_j > 0$ by

choosing $\eta_{jj} = \left\lceil \frac{s_j \rho_j}{H(q)_j} \right\rceil$, then

$s_j \rho_j - H(q)_j \eta_{jj} \text{sign}(s_j) \leq 0$. On the other hand, if

$s_j < 0$, by choosing $\eta_{jj} = -\left\lceil \frac{s_j \rho_j}{H(q)_j} \right\rceil$,

then $s_j \rho_j - H(q)_j \eta_{jj} \text{sign}(s_j) \leq 0$. Thus, through selection of the mentioned parameter, the following equation is resulted:

$$\begin{aligned} \dot{V} &= \sum_{j=1}^n (s_j \rho_j - H(q)_j \eta_{jj} \text{sign}(s_j)) - s^T \tilde{D}(q)Ps \leq -s^T \tilde{D}(q)Ps \leq 0 \end{aligned} \quad (32)$$

If the matrix $\tilde{D}(q)$ and the diagonal matrix P are positive definite, the Eq. (32) is established.

Researchers have proved that the dynamical characteristic of the robot manipulator is in such a way that causes matrix $\tilde{D}(q)$ always becomes positive definite matrix [1]. Thus, if diagonal matrix P is chosen as a positive definite matrix, Eq. (32) is made and the closed-loop system in the presence of all the uncertainties will have the global asymptotic stability.

4. Adaptive Fuzzy Integral Sliding Mode Control

Although the robot manipulator with the proposed control (from the previous section) has the global asymptotic stability in the presence of all uncertainties, occurrence of the undesired chattering phenomenon in the control input is inevitable. Occurrence of the chattering phenomenon causes stimulation of high rank nonlinear dynamics of the

robot manipulator. In this case, guaranty of the closed-loop system stability becomes impossible. To prevent occurrence of the chattering phenomenon, using a MIMO adaptive fuzzy approximator, $\eta \text{sign}(s)$ is approximated in the control input of Eq. (20). Therefore, the structure of this adaptive fuzzy approximator is described as follows:

In Fig. 1, main modules of a fuzzy system are demonstrated. According to this figure, a fuzzy system consists of the following sections modules [11]:

- Fuzzification
- Fuzzy interface engine
- Fuzzy rules base
- Defuzzification

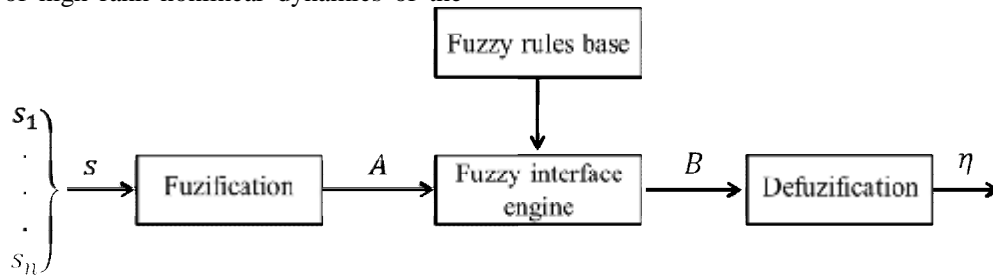


Figure1. Schema of a MIMO fuzzy system.

In design of this fuzzy system, singleton fuzzification, Mamdani fuzzy interface engine, and center average defuzzification are used. The input of fuzzy system is sliding surface vector and the output of fuzzy system is $\eta \in \mathbb{R}^n$ vector. In fact, to prevent occurrence of chattering phenomenon in the control input, by using fuzzy system, approximation of $\eta \in \mathbb{R}^n$ is provided. In this case, due to elimination of discrete part $\eta \text{sign}(s)$ in the control input, occurrence of undesired chattering phenomenon is prevented. Generally, the fuzzy rules of this fuzzy system can be expressed as follows:

$$R^l: \text{If } s_1 \text{ is } A_1^l, s_2 \text{ is } A_2^l, \dots, s_n \text{ is } A_n^l \text{ then } \eta_1 \text{ is } B_1^l, \eta_2 \text{ is } B_2^l, \dots, \eta_n \text{ is } B_n^l \quad (33)$$

where R^l shows l^{th} rule, s_j is j^{th} input fuzzy system, A_j^l is j^{th} membership function of l^{th} rule premise part, η_j is j^{th} output and B_j^l is j^{th} membership function of l^{th} rule result part. Then, the input vector with $s = (s_1, \dots, s_n)^T$ and output vector with $\eta = (\eta_1, \dots, \eta_n)^T$ are shown. The output of fuzzy system, $\eta \in \mathbb{R}^n$ vector, can be expressed as follows:

$$\eta = \frac{\sum_{l=1}^M \theta_{\eta_j}^l \left(\prod_{j=1}^n \mu_{A_j^l}(s_j) \right)}{\sum_{l=1}^M \left(\prod_{j=1}^n \mu_{A_j^l}(s_j) \right)} = \theta_{\eta_j}^T \xi(s) \quad (34)$$

where $\theta_{\eta_j}^T$ is the vector of membership function centers at result part and $\xi(s)$ is the height of this membership function centers. $\theta_{\eta_j}^T$ and $\xi(s)$

vectors can be shown as follows:

$$\theta_{\eta_j}^T = (\theta_{\eta_j^1}, \dots, \theta_{\eta_j^n})^T \quad (35)$$

$$\xi(s) = (\xi^1(s), \dots, \xi^M(s))^T \quad (36)$$

$$\xi^l(s) = \frac{\prod_{j=1}^n \mu_{A_j^l}(s_j)}{\sum_{l=1}^M \left(\prod_{j=1}^n \mu_{A_j^l}(s_j) \right)} \quad (j = 1, \dots, n) \quad (37)$$

In order to make the MIMO fuzzy system membership functions differentiable, they are chosen to be Gaussian:

$$\mu_{A_j^l}(s_j) = \exp \left[-\left(\frac{s_j - \alpha_j^l}{\sigma_j^l} \right)^2 \right] \quad (j = 1, \dots, n) \quad (38)$$

where α_j^l is the center of membership function A_j^l , and σ_j^l is the standard deviation of membership function A_j^l . In this fuzzy system, according to Table 1, seven linguistic variables are considered for inputs s_j and

outputs η_j . Membership functions of these linguistic variables are shown in Figure 2.

Table 1. MIMO fuzzy system output and input vector linguistic variables.

NB	Negative Big
NM	Negative Medium
NS	Negative Small
ZO	Zero
PS	Positive Small
PM	Positive Medium
PB	Positive Big

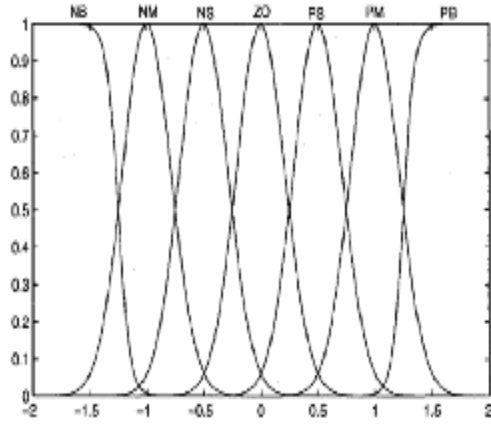


Figure 2. Membership function regarding the linguistic variables of MIMO fuzzy system output and input vector.

Linguistic variable membership functions PB and NB are expressed as follows:

$$\mu_{A_j^i}(s_j) = \frac{1}{1 + [\exp(\frac{s_j - \alpha_j^i}{\sigma_j^i})]^2} \quad (j = 1, \dots, n) \quad (39)$$

According to mentioned points, the adaptive fuzzy integral sliding mode controller is as follows:

$$u(t) = \tilde{D}(q)^{-1} [\dot{q}_d - \hat{F}(q, \dot{q}) - 2\lambda \dot{e} - \lambda^2 e] - Ps - \eta \quad (40)$$

where Z_{η_j} is the positive constant. Derivative of the Lyapunov function in respect to time is as follows:

$$\begin{aligned} \dot{V} &= \frac{1}{2} \dot{s}^T s + \frac{1}{2} s^T \dot{s} + \frac{1}{2} \sum_{j=1}^n \left(\frac{1}{Z_{\eta_j}} \dot{\tilde{\theta}}_{\eta_j}^T \tilde{\theta}_{\eta_j} + \frac{1}{Z_{\eta_j}} \tilde{\theta}_{\eta_j}^T \dot{\tilde{\theta}}_{\eta_j} \right) = s^T \dot{s} + \sum_{j=1}^n \frac{1}{Z_{\eta_j}} \tilde{\theta}_{\eta_j}^T \dot{\tilde{\theta}}_{\eta_j} \\ &= s^T [\rho - \tilde{D}(q)\eta - \tilde{D}(q)Ps] + \sum_{j=1}^n \frac{1}{Z_{\eta_j}} \tilde{\theta}_{\eta_j}^T \dot{\tilde{\theta}}_{\eta_j} = \sum_{j=1}^n (s_j \rho_j - H(q)_j \eta_j) + \sum_{j=1}^n \frac{1}{Z_{\eta_j}} \tilde{\theta}_{\eta_j}^T \dot{\tilde{\theta}}_{\eta_j} - s^T \tilde{D}(q)Ps \\ &\quad - \sum_{j=1}^n (s_j \rho_j - H(q)_j \theta_{\eta_j}^T \xi(s)) + \sum_{j=1}^n \frac{1}{Z_{\eta_j}} \tilde{\theta}_{\eta_j}^T \dot{\tilde{\theta}}_{\eta_j} - s^T \tilde{D}(q)Ps \end{aligned} \quad (48)$$

To design the adaptive fuzzy system that can provide approximated η vector and to prove closed-loop system stability, Eq. (40) is arranged as follows:

$$\ddot{q}_d = \hat{F}(q, \dot{q}) + 2\lambda \dot{e} + \lambda^2 e + \tilde{D}(q)[Ps + \eta + u(t)] \quad (41)$$

From Equations (4), (13), and (41):

$$\dot{s} = \ddot{q} - \ddot{q}_d + 2\lambda \dot{e} + \lambda^2 e = \rho_F + \rho_D u(t) - \tilde{D}(q)Ps - \tilde{D}(q)\eta \quad (42)$$

where ρ_F , ρ_D , and ρ are presented as follows:

$$\begin{cases} \rho_F = F(q, \dot{q}) - \hat{F}(q, \dot{q}) \\ \rho_D = D(q) - \tilde{D}(q) \\ \rho = \lambda \rho_F + \lambda \rho_D u(t) \\ \dot{s} = \rho - \tilde{D}(q)Ps - \tilde{D}(q)\eta \end{cases} \quad (43)$$

In Eq. (43), η vector corresponds with Equation (34). Additionally, it is assumed that $\theta_{\eta_{j,d}}$ is the desirable value which causes $\eta_j = \theta_{\eta_{j,d}}^T \xi(s)$ to approximate $s_j \rho_j$ in such a way that $\delta_j > 0$ (according to Wang theory [11]). Thus, the following equation is provided:

$$|s_j \rho_j - H(q)_j \theta_{\eta_{j,d}}^T \xi(s)| \leq \delta_j \quad (44)$$

where δ_j is the smallest positive constant. Equation of adaptive fuzzy approximator error should be described as below:

$$\tilde{\theta}_{\eta_j} = \theta_{\eta_j} - \theta_{\eta_{j,d}} \quad (45)$$

If Eq. (34) is described as scalar and Eq. (45) is substituted in it, the following equation is obtained:

$$\eta_j = \tilde{\theta}_{\eta_j}^T \xi(s) + \theta_{\eta_{j,d}}^T \xi(s) \quad (46)$$

Furthermore, to prove the closed-loop system stability, Lyapunov candidate function is presented as bellow:

$$V = \frac{1}{2} s^T s + \frac{1}{2} \sum_{j=1}^n \frac{1}{Z_{\eta_j}} \tilde{\theta}_{\eta_j}^T \tilde{\theta}_{\eta_j} \quad (47)$$

$$= \sum_{j=1}^n \left(s_j \rho_j - H(q)_j \tilde{\theta}_{\eta_j}^T \xi(s) - H(q)_j \theta_{\eta_j d}^T \xi(s) \right) + \sum_{j=1}^n \frac{1}{Z_{\eta_j}} \tilde{\theta}_{\eta_j}^T \dot{\theta}_{\eta_j} - s^T \tilde{D}(q) P s$$

$$- \sum_{j=1}^n \left(s_j \rho_j - H(q)_j \theta_{\eta_j d}^T \xi(s) \right) + \sum_{j=1}^n \frac{1}{Z_{\eta_j}} \tilde{\theta}_{\eta_j}^T (\dot{\theta}_{\eta_j} - Z_{\eta_j} H(q)_j \xi(s)) - s^T \tilde{D}(q) P s$$

The adaptive law is chosen as follows:

$$\dot{\tilde{\theta}}_{\eta_j} = Z_{\eta_j} H(q)_j \xi(s) \quad (49)$$

By inserting Eq. (49) in Eq. (48):

$$\dot{V} = \sum_{j=1}^n \left(s_j \rho_j - H(q)_j \theta_{\eta_j d}^T \xi(s) \right) - s^T \tilde{D}(q) P s \quad (50)$$

From Equations (44) and (50):

$$\dot{V} \leq \sum_{j=1}^n \delta_j - s^T \tilde{D}(q) P s \leq \sum_{j=1}^n (\delta_j - H(q)_j P_{jj} s_j^2) \quad (51)$$

In Eq. (51), if $\dot{V} \leq 0$, the main diagonal entries of matrix P are chosen in such ways that fulfill the following equation:

$$H(q)_j P_{jj} s_j^2 \geq \delta_j \quad (52)$$

Thus, closed-loop system with adaptive fuzzy integral sliding mode controller in the presence of all the structured and unstructured uncertainties and also disturbances has the global asymptotic stability. Robot manipulator with the proposed control in the presence of all uncertainties has the global asymptotic stability. However, λ , P (matrices entries), Z_{η_j} coefficients, and existing membership functions in part of fuzzy approximator rules base assumption must be chosen by trial and error. Defining these parameters has a direct relation with control input amplitude and robot manipulator tracking error bound. Hence, in the next section of the paper, the modified harmony search optimization algorithm will be presented for choosing optimal value of these parameters.

5. Optimization Technique

5.1. Original Harmony Search Algorithm

The Harmony Search (HS) algorithm has been inspired by the music improvisation process. It is a relatively recent meta-heuristic optimization technique and has been used to solve various optimization problems. This algorithm was first introduced by Geem et al. [22]. The main idea behind the HS algorithm is to achieve the most harmony among the musicians when they are playing a note. Most

important characteristics of HS algorithm are as follows [23]:

1. Simplicity in concept.
2. Capability of solving both continuous and discontinuous optimization problems.
3. Few adjusting parameters.
4. Easy to implement.
5. Proper trade-off between local and global exploration.

The HS algorithm is a population based optimization algorithm. The first step in this algorithm is to generate a matrix known as Harmony Memory (HM) matrix. Each individual entries of this matrix represent a note which is played by a musician to be improved (improvisation) to achieve the most harmony with the other players. To implement the improvisation process, three rules need to be followed:

1. Memory consideration.
2. Pitch adjustment.
3. Random search.

5.2. Improvisation Through Memory Consideration and Random Research

At this stage, a constant value known as Harmony Memory Considering Rate (HMCR) is defined. Then, a new harmony is created by using HM and HMCR:

$$x_{ij}^{new} = \begin{cases} x_{ij}^{HM} & \text{rand}() < HMCR \\ x_{ij}^{rand} & \text{Otherwise} \end{cases} \quad (53)$$

$$x_i^{HM} = [x_{i1}^{HM}, \dots, x_{id}^{HM}]$$

$$x_i^{rand} = [x_{i1}^{rand}, \dots, x_{id}^{rand}]$$

where x_i^{HM} is the i^{th} individual in the HM matrix and x_i^{rand} shows a random harmony generated in the acceptable range. A large value of HMCR causes the algorithm to form a new harmony from the HM matrix whereas a low value of HMCR causes the algorithm to perform a random exploration.

5.3. Improvisation Through Pitch Adjustment and Random Research

The new harmony constructed in the last step (Harmony Consideration) is checked to decide whether its pitch should be adjusted or not. A parameter known as Pitch Adjusting Rate

(PAR) is defined as follows to simulate the process of pitch adjustment:

$$x_{i,j}^{new} = \begin{cases} x_{i,j}^{HM} \pm rand \times bw ; rand < PAR \\ x_{i,j}^{rand} ; Otherwise \end{cases} \quad (54)$$

Fesanghary et al. shows that the capability of the HS algorithm can be significantly improve by updating the value of bw [24]. Thus, the value of bw is updated as follows during the optimization process:

$$bw(\varphi) = bw_{max} \times \exp(d \times \varphi) \quad (55)$$

$$d = \ln(bw_{min}/bw_{max})/NI$$

In Equation (34), $bw(\varphi)$ represents the bandwidth corresponding to φ^{th} iteration. Similarly, performance of HS algorithm can also be improved by updating the PAR value [24] as follows:

$$PAR(Iter) = PAR_{min} + (PAR_{max} - PAR_{min})/NI \quad (56)$$

The HM matrix is updated by using these steps. The improvisation process will be repeated until the stopping criterion is met.

5.4. Modified HS Algorithm (MHSA)

In this section, a new modification approach is introduced in order to improve the total capability of the algorithm in both local and global exploration. The proposed modification approach increases both the diversity of the HM matrix and the convergence speed of the HS algorithm. The proposed modification method is applied to the HS algorithm after each improvisation step. In this regard, for each solution in the HM (X_i), three different solutions (X_{q1} , X_{q2} , and X_{q3}) are chosen from HM such that $q1 \neq q2 \neq q3 \neq i$. Then, a new improved solution is constructed as follows:

$$X_{Imp} = X_{q1} + \beta_1 \times (X_{q2} - X_{q3}) \quad (57)$$

At this stage, using X_{Imp} , X_i , and X_{best} , three different promising test solutions are generated as follows:

$$X_{Test1,j}^{new} = \begin{cases} X_{Imp,j} ; \beta_1 \leq \beta_2 \\ X_{best,j} ; Otherwise \end{cases} \quad (58)$$

$$X_{Test2,j}^{new} = \begin{cases} X_{Imp,j} ; \beta_2 \leq \beta_3 \\ X_{i,j} ; Otherwise \end{cases} \quad (59)$$

$$X_{Test3} = \beta_4 \times X_{best} + \beta_5 \times (X_{best} - HM(I_{rand})) \quad (60)$$

The X_i in HM is replaced with the best individual among X_{Test1} , X_{Test2} , X_{Test3} and X_i . The HMCR parameter plays an important role in the HS algorithm; especially for increasing speed of the convergence. As it was

mentioned before, a high value of HMCR causes the HS algorithm to move towards selected value from the HM. Whereas a low value is approached toward random movement. Thus, in order to adaptively update the HMCR, after the algorithm is iterated for several times, a new heuristic formulation is defined as follows:

$$HMCR^{\varphi+1} = (1/2NI)^{1/NI} HMCR^{\varphi} \quad (61)$$

In Eq. (61), φ is the iteration number. Generally, a heuristic algorithm like MHSA only requires checking the cost function and no longer requires information about the system. Hence, in this paper, the Mean-Root-Squared Errors (MRSE) is considered as follows:

$$MRSE = E(k) = 1/N \sum_{i=1}^N |\epsilon(i)| + |u(i)| \quad (62)$$

where N represents the number of sample, i is the iteration number, $\epsilon(i)$ denotes the trajectory error of i th sample for the object, and $u(i)$ is the control signal.

6. Advantages of The Proposed Control

Significant innovations in the proposed control design are listed as follows:

1. To define the proposed control sliding surface, error information, error derivative and error integral are used. In this case, according to Eq. (9), by choosing suitable coefficient λ , it is possible that the transient position tracking error of the robot Manipulator converges toward zero in a shorter time. This feature is very important in controlling the position of the welding and assembling robots.
2. In many articles, the robot manipulator position tracking control in torque space has been presented. In design of these controllers, the dynamic equations of the robot manipulator actuators have not been considered. Thus, guarantee of the closed-loop stability system in the presence of actuators is difficult and in some cases might be impossible [14,16,19]. However, in design of the proposed method, dynamics of actuators have been included.
3. In many adaptive fuzzy sliding mode controllers, presented for tracking the robot manipulator, to reduce the tracking error, some coefficients have been considered. The controllers can reduce the tracking error by increasing these coefficients, however an increase in these coefficients

causes an increase in the amplitude of control input. This causes saturation of actuators [11,13,14]. In the adaptive law of the proposed method, the coefficient Z_{m_i} has been used. Increasing of this coefficient causes reduction of tracking error, while it does not have any influence in increasing of control input amplitude. This advantage is shown in the simulation section.

4. In SISO adaptive fuzzy sliding mode control that is presented for robot manipulator position tracking, the influence that robot manipulator joints apply on each other is disregarded [14]. However, if the robot manipulator intends to operate with high speed, influence of the joints on each other exists significantly. Thus, it is possible to make the stability of closed-loop system very difficult. In design of the proposed adaptive fuzzy approximator, MIMO fuzzy rule has been used. Thus, reciprocal influence of robot manipulator joints can be reduced by choosing suitable fuzzy rules.
5. In most papers which are presented for robot manipulator controller, there is no proving for stability of closed-loop system [20, 21]. However, in this paper, it is proved that the closed-loop with purposed controller system has the global asymptotic stability in the presence of all uncertainties.
6. The use of the inverse dynamic technique causes the uncertainty bounds to be reduced. Hence, the amplitude of the control input can be performed in a desired range for determination of the control input coefficients [25,26].
7. In the proposed control design, to define the control input parameters, modified optimization algorithm has been used. In this case, increment of the control input amplitude is prevented and implementation of the proposed control becomes much more cost-efficient.

7. Case Studies

In 1981, Sankyo Seiki, Pentel and NEC presented a completely new concept for assembly robots. The robot was developed under the guidance of Hiroshi Makino, a professor at the University of Yamanashi. This robot was called Selective Compliance

Assembly Robot Arm (SCARA). Its arm was rigid in the Z-axis and pliable in the XY-axes, which allowed it to be adapted to holes in the XY-axes [18]. By virtue of the SCARA's parallel-axis joint layout, the arm is slightly compliant in the X-Y direction but rigid in the 'Z' direction. Hence the term: Selective Compliant was applied for the system. This is advantageous for many types of assembly operations, i.e., inserting a round pin in a round hole without binding. The second attribute of the SCARA is the jointed two-link arm layout similar to our human arms, hence the often-used term, Articulated. This feature allows the arm to extend into confined areas and then retract or "fold up" out of the way. This is advantageous for transferring parts from one cell to another or for loading/unloading process stations that are enclosed. In this section, Fig. 3 is used as a case study to examine performance of the proposed controllers of the SCARA robot manipulator. Considering Eq. (1), dynamic equations of the robot manipulator in the presence of PMDC motor's dynamics, are as follows [1]:

$$\begin{aligned}
 M(q) &= \begin{bmatrix} M_{11} & M_{12} & M_{13} \\ M_{21} & M_{22} & M_{23} \\ M_{31} & M_{32} & M_{33} \end{bmatrix} \\
 M_{11} &= l_1^2 \left(\frac{m_1}{3} + m_2 + m_3 \right) + l_1 l_2 (m_2 + 2m_3) \cos(q_2) + l_1^2 \left(\frac{m_2}{3} + m_3 \right) + \frac{J_{m1}}{r_1^2} \\
 M_{12} &= M_{21} = -l_1 l_2 \left(\frac{m_2}{3} + m_3 \right) \cos(q_2) - l_2^2 \left(\frac{m_2}{3} + m_3 \right) \\
 M_{22} &= l_2^2 \left(\frac{m_2}{3} + m_3 \right) + \frac{J_{m2}}{r_2^2} \\
 M_{33} &= m_3 + \frac{J_{m3}}{r_3^2} \\
 M_{13} &= M_{23} = M_{31} = M_{32} = 0 \\
 C(q, \dot{q}) &= l_1 l_2 \sin(q_2) \begin{bmatrix} C_{11} & C_{12} & C_{13} \\ C_{21} & C_{22} & C_{23} \\ C_{31} & C_{32} & C_{33} \end{bmatrix} \\
 C_{11} &= -\dot{q}_2 (m_2 + 2m_3) \\
 C_{12} &= C_{22} = -\dot{q}_2 \left(\frac{m_2}{2} + m_3 \right) \\
 C_{13} &= C_{22} = C_{23} = C_{31} = C_{32} = C_{33} = 0 \\
 B &= \begin{bmatrix} B_{11} & B_{12} & B_{13} \\ B_{21} & B_{22} & B_{23} \\ B_{31} & B_{32} & B_{33} \end{bmatrix} \\
 B_{11} &= (E_{m_1} + K_{b_1} K_{m_1} / R_1) / r_1^2 \\
 B_{22} &= (E_{m_2} + K_{b_2} K_{m_2} / R_2) / r_2^2 \\
 B_{33} &= (E_{m_3} + K_{b_3} K_{m_3} / R_3) / r_3^2
 \end{aligned}$$

$$B_{13} = B_{22} = B_{23} = B_{31} = B_{32} = 0 \quad (63)$$

$$K = \begin{bmatrix} K_{11} & K_{12} & K_{13} \\ K_{21} & K_{22} & K_{23} \\ K_{31} & K_{32} & K_{33} \end{bmatrix}$$

$$K_{11} = K_{m_1}/(R_1 + r_{-1})$$

$$K_{22} = K_{m_2}/(R_2 + r_{-2})$$

$$K_{33} = K_{m_3}/(R_3 + r_{-3})$$

$$K_{13} = K_{22} = K_{23} = K_{31} = K_{32} = 0$$

$$G(q) = \begin{bmatrix} 0 \\ 0 \\ -m_3 g \end{bmatrix}$$

$$F_d = \begin{bmatrix} 2 & 0 & 0 \\ 0 & 2 & 0 \\ 0 & 0 & 2 \end{bmatrix}, \quad F_s = \begin{bmatrix} 1 \\ 1 \\ 1 \end{bmatrix}$$

$$\tau_{dl} = \begin{bmatrix} 5 \sin(t) \\ 5 \sin(t) \\ 5 \sin(t) \end{bmatrix} + \begin{bmatrix} \sin(t) \\ \sin(t) \\ \sin(t) \end{bmatrix}$$

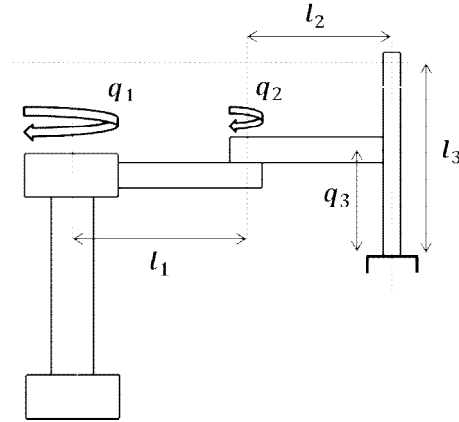


Figure 3. The SCARA robot manipulator.

SCARA robot manipulator and PMDC motor parameters are shown in Table 2.

Table 2. SCARA robot manipulator and PMDC motor parameters.

Parameter	Value	Parameter	Value
l_1	0.75 m	B_{m_2}	1×10^{-2}
l_2	0.5 m	B_{m_3}	1×10^{-2}
l_3	1 m	K_{b_1}	$1 \times 10^{-2} \text{ volt}/(\text{rad}/\text{sec})$
m_1	5 kg	K_{b_2}	$1 \times 10^{-2} \text{ volt}/(\text{rad}/\text{sec})$
m_2	3 kg	K_{b_3}	$1 \times 10^{-2} \text{ volt}/(\text{rad}/\text{sec})$
m_3	2 kg	K_{m_1}	$1 \times 10^{-2} \text{ Nm/A}$
J_{m_1}	$1 \times 10^{-4} \text{ kgm}^2$	K_{m_2}	$1 \times 10^{-2} \text{ Nm/A}$
J_{m_2}	$1 \times 10^{-4} \text{ kgm}^2$	K_{m_3}	$1 \times 10^{-2} \text{ Nm/A}$
J_{m_3}	$1 \times 10^{-4} \text{ kgm}^2$	R_1	1 Ω
r_{-1}	1×10^{-2}	R_2	1 Ω
r_{-2}	1×10^{-2}	R_3	1 Ω
r_{-3}	1×10^{-2}	g	9.8 N/kg
B_{m_1}	1×10^{-2}		

where l_1 , l_2 , and l_3 are the length of the links; m_1 , m_2 , and m_3 are the mass of the first, second and third link, respectively; g is the acceleration of gravity; J_{m_1} , J_{m_2} and J_{m_3} are the inertial of the Motors; r_1 , r_2 and r_3 are the gears ratio; B_{m_1} , B_{m_2} and B_{m_3} are the friction

of the motors; K_{b_1} , K_{b_2} , and K_{b_3} are *emf* constant of motors recursive; K_{m_1} , K_{m_2} and K_{m_3} are constant of motors torque; and R_1 , R_2 and R_3 are the motors armature resistance.

Desirable trajectory is introduced by Eq. (54) and desirable positions of joints 1, 2 and 3 are

shown in Fig. 4. Fuzzy rules base systems are adjusted the same as Fig. 1, according to Eq.

(33) and membership functions of these rules. The initial conditions of the robot manipulator joints are considered equal to

$$\begin{aligned} [q_1(0) \quad q_2(0) \quad q_3(0)]^T &= [0.1 \quad 0.1 \quad 0.1]^T \\ \begin{bmatrix} \ddot{q}_{d1} \\ \ddot{q}_{d2} \\ \ddot{q}_{d3} \end{bmatrix} &= \begin{bmatrix} -4 & 0 & 0 \\ 0 & -4 & 0 \\ 0 & 0 & -4 \end{bmatrix} \times \begin{bmatrix} \dot{q}_{d1} \\ \dot{q}_{d2} \\ \dot{q}_{d3} \end{bmatrix} + \\ &\begin{bmatrix} -4 & 0 & 0 \\ 0 & -4 & 0 \\ 0 & 0 & -4 \end{bmatrix} \times \begin{bmatrix} q_{d1} \\ q_{d2} \\ q_{d3} \end{bmatrix} + \\ &\begin{bmatrix} 3 & 0 & 0 \\ 0 & 3 & 0 \\ 0 & 0 & 3 \end{bmatrix} \times \begin{bmatrix} 1 - 0.6T \\ 1 - 0.8T \\ 1 - 1.2T \end{bmatrix} \\ \ddot{q}_d &= \begin{bmatrix} \ddot{q}_{d1} \\ \ddot{q}_{d2} \\ \ddot{q}_{d3} \end{bmatrix}; \dot{q}_d = \begin{bmatrix} \dot{q}_{d1} \\ \dot{q}_{d2} \\ \dot{q}_{d3} \end{bmatrix}; q_d = \begin{bmatrix} q_{d1} \\ q_{d2} \\ q_{d3} \end{bmatrix} \quad (64) \end{aligned}$$

In the mentioned equation, values \ddot{q}_d , \dot{q}_d , and q_d are desirable acceleration vector, desirable velocity vector, and desired positional vector of robot manipulator joints, respectively. Function T also is a square pulse with 1 amplitude, 2 second period, pulse width 50 % of period and 0 second phase delay.

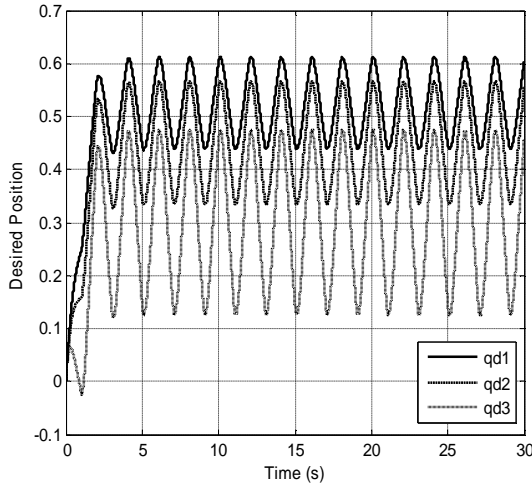


Figure 4. Desired position of the first, second and third joints of the SCARA robot manipulator.

In this part the proposed controller, five-staged examination is performed. In these stages, the proposed controller encounters with various challenges. Additionally, robustness of the

proposed controller is evaluated against structured and unstructured uncertainties.

Simulation 1: In this simulation, the integral sliding mode position tracking controller is applied to the SCARA robot manipulator. In this simulation, it is assumed that accurate information of SCARA robot manipulator dynamics is available. In other words, the controller is not encountered with uncertainty. To adjust the values of the controller coefficients, the Table 3 is used.

Table 3. Coefficients of integral sliding mode controller.

Parameter	Value	Parameter	Value
λ_1	10	P_2	30
λ_2	12	η_{11}	30
λ_3	10	η_{22}	50
P_1	50	η_{33}	80
P_2	20		

After running the simulation, according to Fig. 5, the first, second and third joint position tracking errors have converged from initial value of 0.1 towards zero in a short time. As expected, due to lack of uncertainty, the closed-loop system does not have steady-state error. Motor input voltage amplitude of the first, second and third of robot manipulator are shown in the Figs. 6, 7 and 8, respectively. From these figures, the amplitude of input controls are situated in an acceptable limit. However, due to occurrence of undesired chattering phenomenon, practical implementation of this controller becomes problematic.

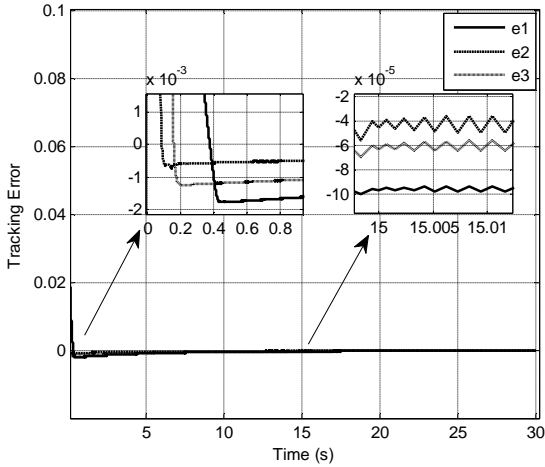


Figure 5. Tracking errors of the first, second and third joint due to applying the integral sliding mode controller.

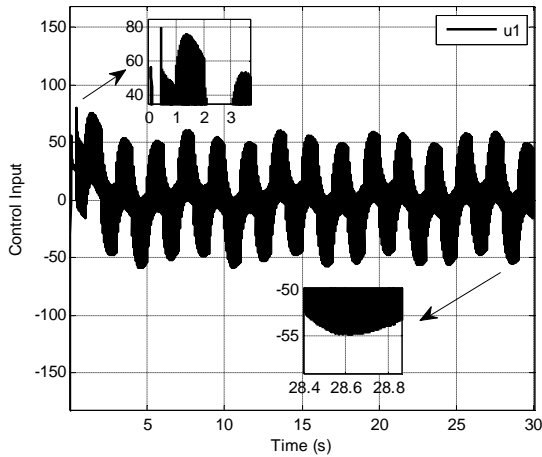


Figure 6. The first motor input voltage due to applying the integral sliding mode controller.

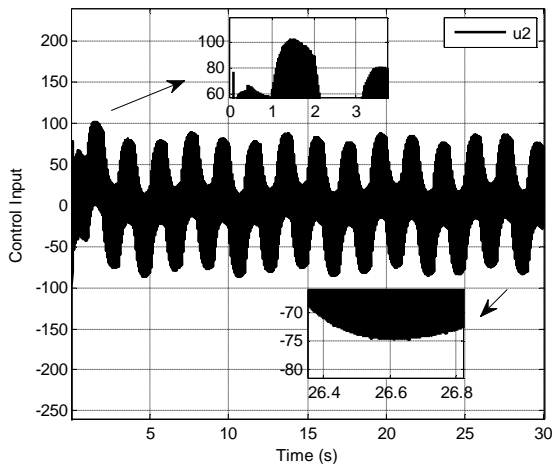


Figure 7. The second motor input voltage due to applying the integral sliding mode controller.

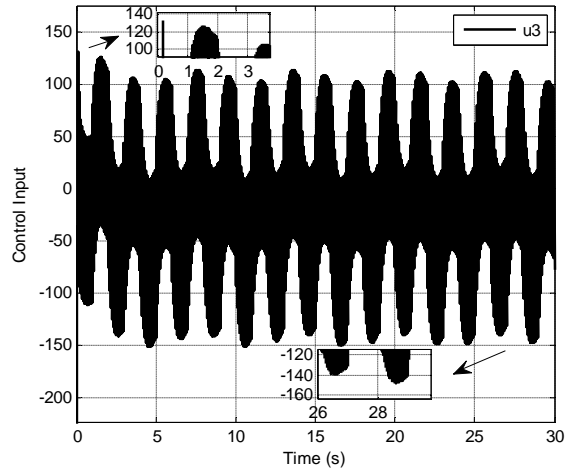


Figure 8. The third motor input voltage due to applying the integral sliding mode controller.

Simulation 2: In this stage of the simulation, the integral sliding mode control is confronted with a more serious challenge. In this part, it is assumed that the information regarding the dynamics of static friction, dynamic friction, disturbance and dynamics of SCARA robot manipulator PMDC motors are not available. Additionally, known parameters of the robot manipulator are shown in Table 4. In other words, in this part of simulation, the integral sliding mode controller is encountered with structured and unstructured uncertainties. Moreover in this simulation, coefficients of the integral sliding mode controller are adjusted according to Table 3.

Table 4. Known parameters of SCARA robot manipulator.

Parameter	Value	Parameter	Value
\hat{l}_1	0.6 m	\hat{m}_2	2.8 kg
\hat{l}_2	0.4 m	\hat{m}_3	1.8 kg
\hat{l}_3	0.9 m	\hat{g}	9.5 N/kg
\hat{m}_1	4.8 kg		

After running the simulation according to Fig. 9, position tracking errors of the first, second and third joints are converged toward zero in a limited time. However, Figs. 10, 11, and 12 show that the motors input voltages have high chattering phenomenon. Thus, the integral

sliding mode controller is compelled to increase the chattering in control input in order to maintain the stability of the closed-loop system against structured and unstructured uncertainties. Hence, in this case, practical implementation of this controller becomes even more problematic.

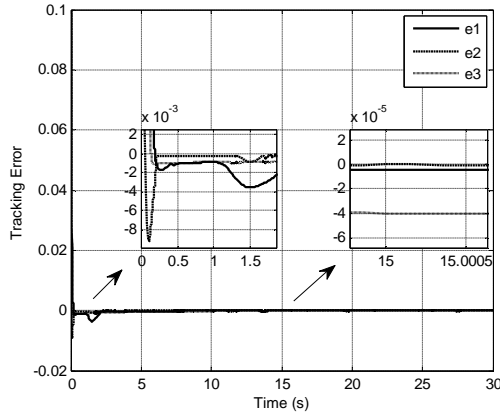


Figure 9. Tracking errors of the first, second and third joint due to the integral sliding mode controller in presence of structured and unstructured uncertainties.

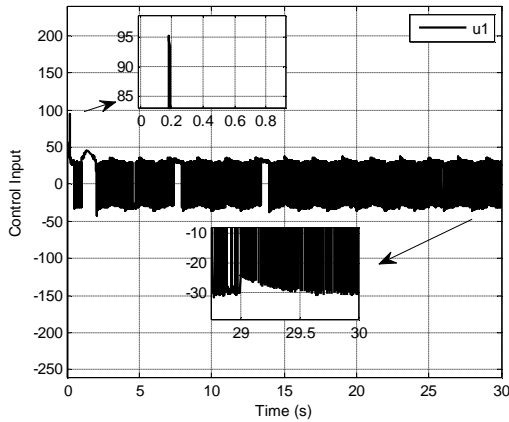


Figure 10. The first motor input voltage due to applying the integral sliding mode controller in the presence of structured and unstructured uncertainties.

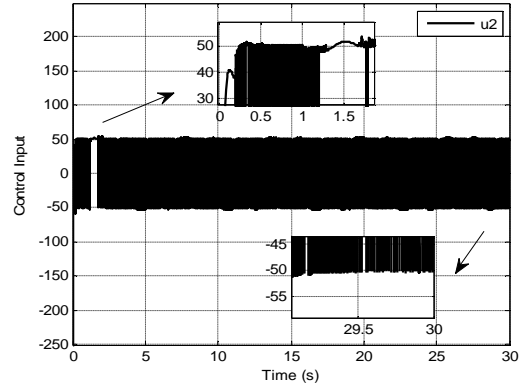


Figure 11. The second motor input voltage due to applying the integral sliding mode controller in the presence of structured and unstructured uncertainties.

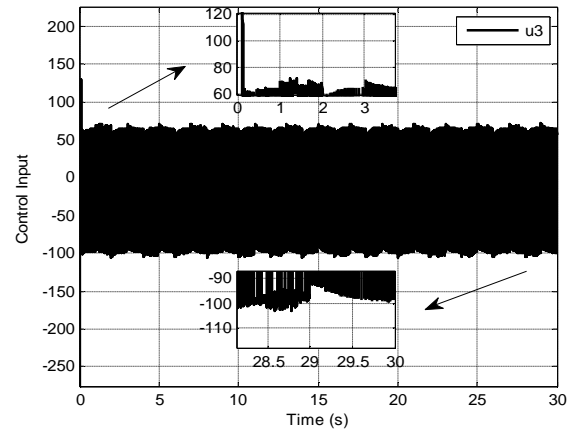


Figure 12. The third motor input voltage due to applying the integral sliding mode controller in the presence of structured and unstructured uncertainties.

Simulation 3: In this part, optimal adaptive fuzzy integral sliding mode position tracking controller is applied to SCARA robot manipulator. Governing condition of this simulation is the same as Simulation 1. According to Table 5, optimal adaptive fuzzy integral sliding mode controller coefficients are adjusted.

Table 5. Coefficients of optimal adaptive fuzzy integral sliding mode controller.

Parameter	Value	Parameter	Value
λ_1	8.7	P_2	28.26
λ_2	11.35	Z_{η_1}	101.14
λ_3	6.98	Z_{η_2}	986.89
P_1	48.87	Z_{η_3}	590.41
P_2	19.04		

Comparing Tables 3 and 5, values for matrix A and P are not chosen the same in both controllers. The parameters of Table 5 also are defined through modified HS optimization algorithm. After running the simulation, Fig. 13 shows the proposed controller performs desirably and joint position tracking errors of the first, second and third converge toward zero in a short time. Figure 14 shows that undesired chattering effects are eliminated in motor input voltage of the first, second and third by using adaptive fuzzy approximator. Additionally, maximum amplitude of motor input voltage first, second and third, are 45.16, 51.89 and 46.06 volts, respectively. Maximum input of the motor voltages are not increased compared to the previous simulations. Figure 15 illustrates that the optimal adaptive fuzzy approximator performs desirably and the values of η_1 , η_2 , and η_3 are approximated in such a way that can guarantee the closed-loop systems stability.

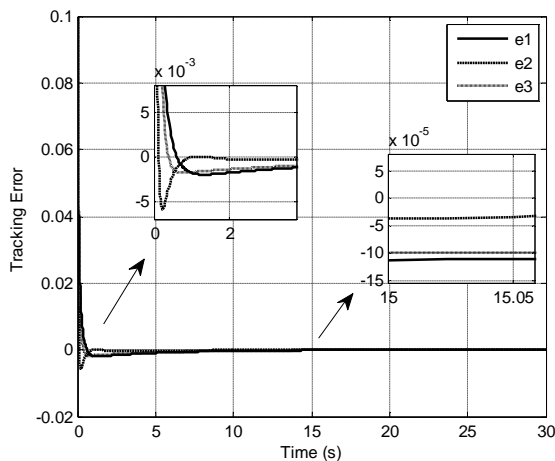


Figure 13. Tracking errors of the first, second and third joint due to applying the optimal adaptive fuzzy integral sliding mode controller.

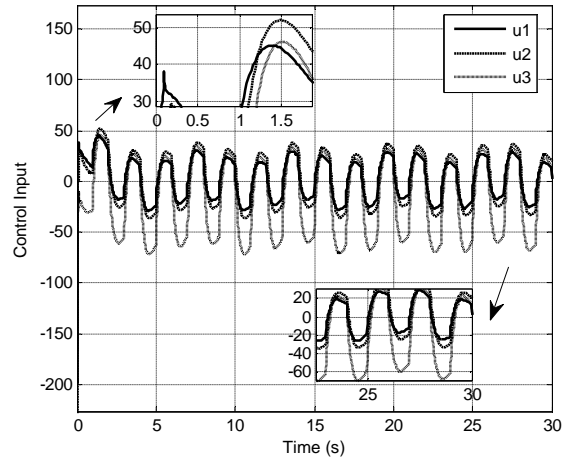


Figure 14. The input voltages of the motors due to applying the optimal adaptive fuzzy integral sliding mode controller.

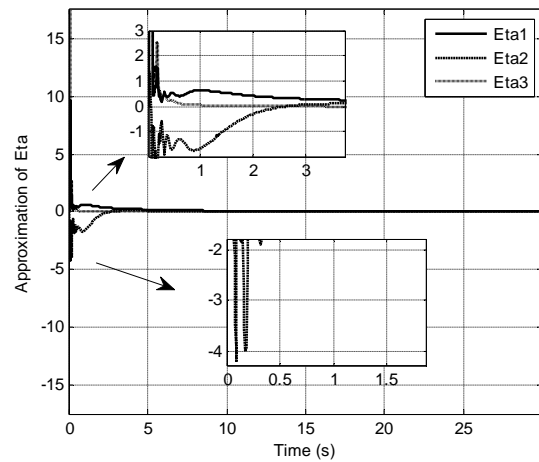


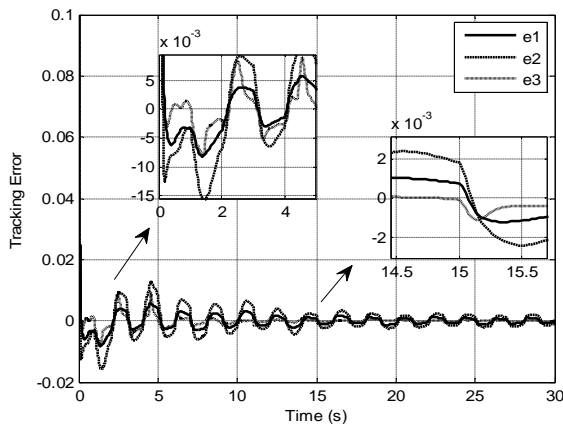
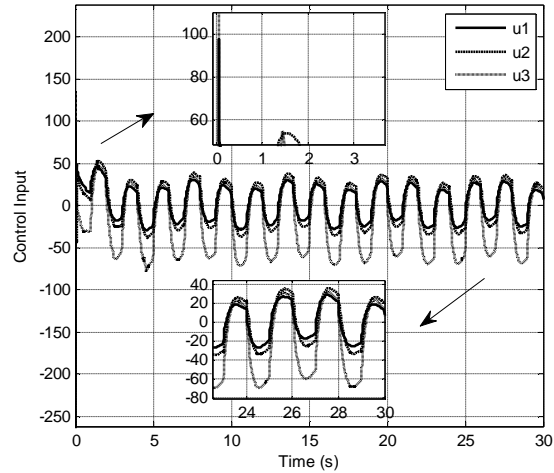
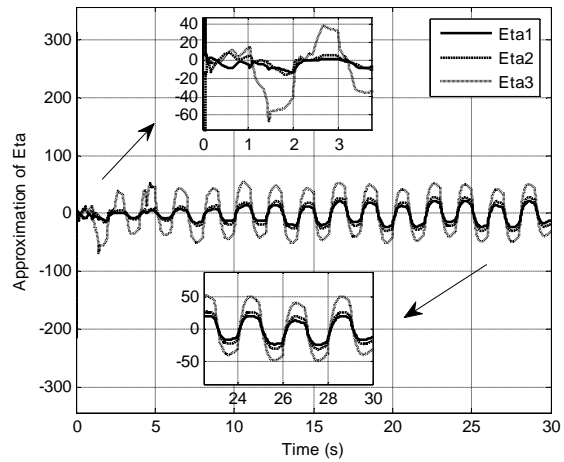
Figure 15. The η_1 , η_2 , and η_3 are outputs of optimal adaptive fuzzy approximator. The symbol η is representing Eta.

Simulation 4: In this part, position tracking controller of optimal adaptive fuzzy integral sliding mode is situated under a great challenge. Thus, in this stage, the proposed control in the SCARA robot manipulator controlling is confronted with the structured and unstructured uncertainties. The proposed control coefficients are adjusted according to Table 6. The existing parameters of Table 6 are defined by modified HS optimization algorithm.

Table 6. Coefficients of optimal adaptive fuzzy integral sliding mode controller in the presence of structured and unstructured uncertainties.

Parameter	Value	Parameter	Value
λ_1	9.82	P_3	31.56
λ_2	13.74	z_{η_1}	105.04
λ_3	8.36	z_{η_2}	1010.78
P_1	52.45	z_{η_3}	600.41
P_2	22.08		

After running the simulation, the proposed controller performs desirably (Fig. 18) and the position tracking errors of the first, second and third joint converges toward zero. However, due to existence of the structured and unstructured uncertainties with large bound, tracking errors are partially increased in comparison with the third simulation. In Fig. 17, undesired chattering phenomenon effects in input voltage of the first, second and third motor are eliminated by optimal adaptive fuzzy approximator. Additionally, maximum amplitude of input voltage of first, second and third motor are 97.08, 53.14, and 137 volts, respectively. In comparison with Simulations 1 and 2, the maximum inputs of motor voltages are not increased. There is just a partial increment that can be seen in comparison with Simulation 3. Moreover, Figure 18 shows that the optimal adaptive fuzzy approximator performs desirably. Additionally, it approximates values η_1 , η_2 , and η_3 in such a way that can guarantee stability of the closed-loop system in spite of the structured and unstructured uncertainties.

**Figure 16.** Tracking errors of the first, second and third joint due to the optimal adaptive fuzzy integral sliding mode control in the presence of structured and unstructured uncertainties.**Figure 17.** The input voltages of the motors due to applying the optimal adaptive fuzzy integral sliding mode controller in the presence of structured and unstructured uncertainties.**Figure 18.** The η_1 , η_2 and η_3 are outputs of optimal adaptive fuzzy approximator in the presence of structured and unstructured uncertainties. The symbol η presents Eta.

Simulation 5: In this section, the adaptive fuzzy sliding mode controller [15] is simulated in order to position control of SCARA manipulator. It should be noted that this simulation is only performed and presented in order to consider and compare with the proposed controller. In order to present a fair comparison, similar to Simulation 4, there are no available information about the existing disturbances, statistical friction dynamics, PMDC motor dynamics, and dynamical friction. Thus in design of the controller [15],

these dynamics are not considered. The known parameters of robot manipulator (that are used in design of the controller) are determined according to Table 4 and 7.

Table 7. Coefficients of adaptive fuzzy sliding mode controller[15] in the presence of structured and unstructured uncertainties.

Parameter	Value	Parameter	Value
λ_1	14	P_3	34
λ_2	14		
λ_3	14		
P_1	54		
P_2	25		

After performing the simulation, tracking error of the joints from initial condition 0.1 are converged to zero according to Figure 19. It can be concluded from comparing Figures (16) and (19) that converging speed of joints tracking errors, in the first 5 seconds of simulation is slower in comparison with Simulation 4. However, it has less steady-state error. It should be noted that after spending 15 seconds, steady-state error of joints converges to zero according to Figure (16). However, according to Figure (20), the controller [15] cannot eliminate effects of undesired chattering phenomenon in first, second, and third motors input voltage. Additionally, maximum input voltage amplitude of motors 1, 2, and 3 are 77.08, 152, and 350 volts, respectively.

Through comparison of Figures (17) and (20), the proposed control input amplitude is much less than controller [15]. Thus, in case of using controller [15], applying motors with higher power are inevitable. Therefore, practical implementation of this controller with motors are very difficult. Additionally, due to appearance of chattering phenomenon in the controller input [15], the life time of these motors will be less. According to Figure (21), the adaptive fuzzy approximator estimates the values of η_1 , η_2 , and η_3 in such a way that the stability of the closed-loop system is guaranteed in the presence of all the structured and unstructured uncertainties. Table (8) is presented in order to clarify performances of Simulations (4) and (5).

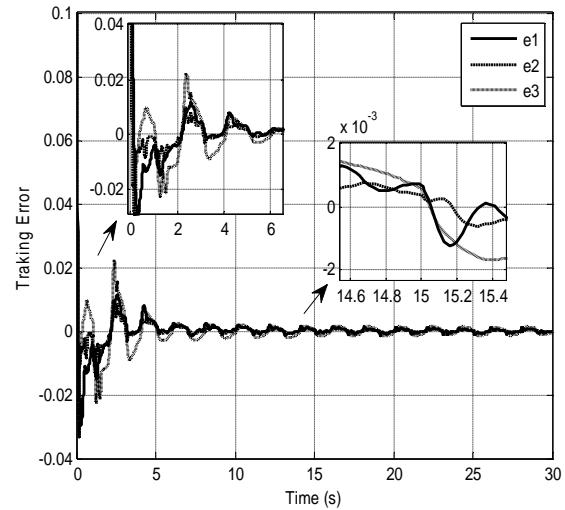


Figure 19. tracking errors of the first, second and third joint due to the adaptive fuzzy sliding mode control[15] in the presence of structured and un-structured uncertainties.

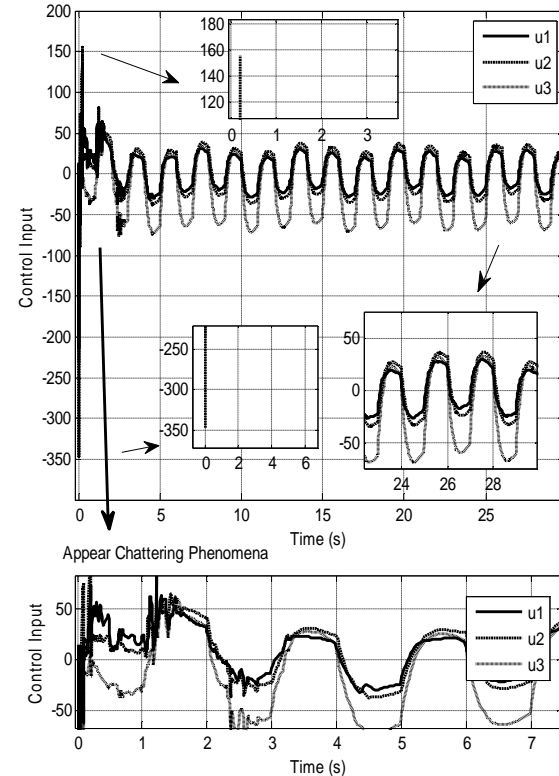


Figure 20. The motors' input voltages due to applying the adaptive fuzzy sliding mode control [15] in presence of structured and un-structured uncertainties.

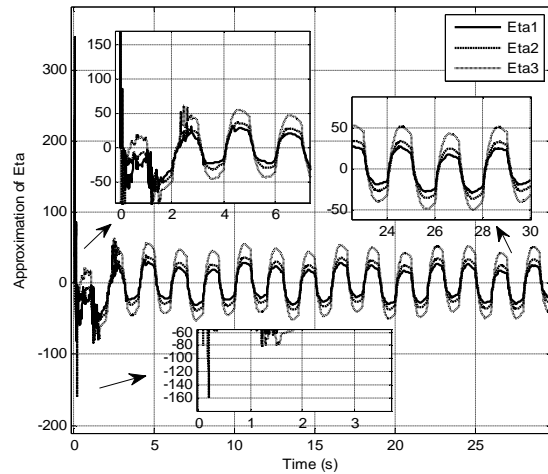


Figure 21. The η_1 , η_2 and η_3 are outputs of adaptive fuzzy approximator[15] in presence of structured and un-structured uncertainty. The symbol η is representing Eta

Table 8.Comparison of performance of the proposed controller and adaptive fuzzy sliding mode controller[15].

Adaptive fuzzy sliding mode controller	Maximum of control input bound	Maximum of transient tracking error with 10^{-3} preciseness	Maximum of control input steady amplitude	Maximum of steady tracking error with 10^{-3} preciseness	Chattering effects
Proposed	137	0.006	67.4	0.0022	eliminate
[15]	350	0.04	72.8	0.0018	remained

Table (8) shows the performance of the proposed controller is more desirable in comparison with controller [15] except in steady tracking error, that controller [15] is slightly more desirable. Amplitude of the proposed controller is much less than controller [15] and there is no trace of chattering in the proposed control input. Thus the practical implementation of the proposed controller is simpler and much more cost-efficient in comparison with controller [15].

8. Conclusions

In this paper, using the inverse dynamic technique and sliding mode control, an integral sliding mode controller was presented to position tracking of the robot manipulator in the presence of motor dynamics. The inverse dynamic technique reduced uncertainties bound. However, due to the application of sliding mode control, the control input was accompanied with occurrence of undesired chattering phenomenon. To

overcome the chattering phenomenon, a MIMO adaptive fuzzy approximator was designed to approximate bound of the remaining uncertainties. Using the integral sliding mode control causes the robot manipulator position tracking error converges toward zero in a very short time. Using MIMO fuzzy system causes reduction of interactions between robot manipulator joints in position tracking of robot manipulator control. Analytical results showed that the closed-loop system with the proposed control has the global asymptotic stability in the presence of all the uncertainties. To prevent increment in the control input amplitude, choosing the coefficients of the control input was performed by modified harmony search optimization algorithm. Simulation results showed desired performance of the proposed control in the position tracking control of SCARA robot manipulator.

1. Reference

- [1] Spong . M.W. , Hutchinson, S., Vidyasagar, M.: Robot Modeling & Control .John Wiley & Sons .(2006)
- [2] Slotine, J.J.E., Li, W. : Applied Nonlinear control , Prentice Hall. (1991)
- [3] . Soltanpour, M. R., Siah, M.: Robust control of robot manipulator in task space. International Journal of Applied and Computational Mathematics. 8(2), 227-238(2009)
- [4] Soltanpour , M. R., Fateh, M. M., Ahmadifard , A. R.: Nonlinear tracking control on a robot manipulator in the task space with uncertain dynamics. Journal of Applied Sciences, Asian Network for Scientific Information. 8,(23), 4397-4403(2008)
- [5] Soltanpour, M. R., Fateh, M. M.: Sliding mode robust control of robot manipulators in the task space by support of feedback linearization and backstepping control. World Applied Sciences Journal. 6(1), 70-76 (2009)
- [6] Shafiei ,S. E., Soltanpour, M. R.: Neural Network Sliding-Model-PID Controller Design for Electrically Driven Robot Manipulators. International Journal of Innovative Computing, Information and Control. 5(12), 3949–3960(2011)
- [7] Khooban, M. H. ,Soltanpour ,M. R.: Swarm Optimization Tuned Fuzzy Sliding Mode Control Design for a Class of Nonlinear Systems in Presence of Uncertainties. Journal of Intelligent and Fuzzy Systems.24(2), 383-394(2013)
- [8] Niknam, T., Khooban, M. H., Soltanpour, M. R.: An Optimal Type II Fuzzy Sliding Mode Control Design for a Class of Nonlinear Systems. Journal of Nonlinear Dynamics. 75(1-2), 73-83(2013)
- [9] Lin, C.M. , Hsu, C.F.: Adaptive fuzzy sliding mode control for induction servo motor systems. IEEE Transactions on Energy Conversion. 19(2), 362–368(2004)
- [10] Wang, L. X. : A Course in Fuzzy Systems and Control. Prentice Hall, Englewood Cliffs, NJ, (1997)
- [11] Yoo, B., Ham, W.: An Adaptive Control Of Robot Manipulator Use Fuzzy Compensator. IEEE Transactions On Fuzzy Fuzzy System. 8(2), 186-199 (2000)
- [12] Wang, J., Rad, A.B., Chan, P.T.: Indirect adaptive fuzzy sliding mode control: Part I: fuzzy switching. Fuzzy Sets and Systems. 122(1), 21–30(2001)
- [13] Guo, Y., Woo, P.Y.: An adaptive fuzzy sliding mode controller for robotic manipulators. IEEE Transactions on Systems, Man, and Cybernetics, Part A: Systems and Humans. 33(2), 149–160(2003)
- [14] Wai, R.J., Lin, C.M., Hsu, C.F.: Adaptive fuzzy sliding mode control for electrical servo drive', Fuzzy sets and systems. 143(2), 295–310(2004)
- [15] Medhaffar, H. ,Derbel, N., Damak, T.: A Decoupled Fuzzy Indirect Adaptive Sliding Mode Control With Application With Robot Manipulator . Int , J . Modeling , Identification And Control . 1(1), 23-29 (2006).
- [16] Soltanpour, M. R., Khalilpour, J., Soltani, M.: Robust Nonlinear Control of Robot Manipulator with Uncertainties in Kinematics, Dynamics and Actuator Models. International Journal of Innovative Computing, Information and Control. 8(6), 5487- 5498(2012)
- [17] Westerlund, L. :The Extended Arm of Man: A History of Industrial Robot. Informationsförlaget Ltd (2000)
- [18] Takosoglu, J. E., Laski, P. A., Blasiak, S.: A fuzzy controller for the positioning control of an electro-pneumatic servo-drive. Proceedings of the Institution of Mechanical Engineers Part I-Journal of Systems and Control Engineering. 226(10), 1335-1343(2012)
- [19] Takosoglu, J. E., Dindorf, R. F., Laski, P. A.:Rapid prototyping of fuzzy controller pneumatic servo-system. International Journal of Advanced Manufacturing Technology. 40(3-4), 349-361(2009)
- [20] Veysi, M., Soltanpour, M. R., Khooban, M. H. : A Novel Self-Adaptive Modified Bat Fuzzy Sliding Mode Control of Robot Manipulator in Presence of Uncertainties in Task Space. Accepted for publication in Journal of Robotica. (2014)
- [21] Soltanpour, M. R., Otadolajam, P., Khooban, M. H. : A New and Robust Control Strategy for Electrically Driven Robot Manipulators: Adaptive Fuzzy Sliding Mode. Accepted for Publication in IET Science, Measurement & Technology Journal.(2014)